15th Australasian Fluid Mechanics Conference
The University of Sydney, Sydney, Australia
13-17 December 2004

CFD Investigation of Particle Deposition Around Bends in a Turbulent Flow

By A. Hossain and J. Naser

School of Engineering and Science, Swinburne University of Technology
PO Box 218, Hawthorn, VIC 3122, AUSTRALIA

Abstract

A comprehensive 3D numerical investigation of hydrodynamics of particles flowing through a horizontal pipe loop consisting of four bends has been modeled. The multiphase mixture model available in Fluent 6.1 [6] is used in this study. In this numerical simulation five different particles have been used as secondary phases to calculate real multiphase effect in which inter-particle interaction has been accounted. The deposition of particles, along the periphery of the wall around bends has been investigated. The effect of bend and fluid velocity on particle deposition has also been investigated. The maximum particle deposition is at the bottom wall in the pipe before entering the bends conversely, downstream of bends the maximum deposition is not at the bottom - as seen upstream of the bends - rather it occurs at an angle of 60^0 toward the inner side from the bottom. The larger particles clearly showed deposition near the bottom of the wall except downstream of the bends. As expected, the smaller particles showed less tendency of deposition and this is more pronounced at higher velocity. This numerical investigation showed good agreement with the experimental results conducted by CSIRO team [9].

Introduction

Particle deposition from flowing suspensions is an important process in various fields of engineering and in nature. Analyzing diminutive suspended particles deposition in fluid streams has attracted considerable attention in the past few decades [1-4,9-11,13,19,20]. This is because of particle deposition plays a major role in a number of industrial processes such as filtration, separation, particle transport, combustion, air and water pollution, and many others.

The CFD (computational fluid dynamics) models to simulate the hydraulic behavior of water-distribution systems have been available for many years [10,11,17]. More recently these models have been extended to analyze water quality as well [10,11]. But at earlier days numerical computations were suffered from some serious limitations. The number of particles is one of them, which was fairly small in numerical simulations, and therefore, size effects can become important, especially with low volume fraction. In this study we have introduced water as a primary and 5 different solid spherical particles as secondary phases. The driving force behind this trend is the timely challenge to comply with increasingly stringent governmental regulations and customer-oriented expectations. Modern management of water-distribution systems like South East Water Ltd, Melbourne Water, Sydney Water, need simulation models that are able to accurately predict the hydrodynamics of particles behavior (cause of dirty water) in the water distribution networks around bends. Particle deposition on pipe-surfaces in turbulent flows had attracted the interest of many researchers. Using the stopping distance of a particle near a wall, Friendlander and Johnstone [8] developed the free-flight model for particle deposition process. Davies [5] among others offered an improved theoretical model for particle deposition rate. Liu and Agarwal [15] analyzed the deposition of aerosol particles in turbulent pipe flows. Simplified simulation procedures for deposition of particles in turbulent flows were described by Abuzeid [1], and Li and Ahmadi [14].

Hossain et al [11] represented the circumferential particle deposition in a straight pipe for turbulent flow in which researchers explained the circumferential particle deposition for a straight pipe. But that model is not applicable for circumferential deposition and hydrodynamic behavior of particles around bends. Particle deposition around bends of a circular cross section is important to the sampling and transport of particles in high-purity fluid streams [4,21]. In the recent experimental study Pui [4] revealed that discrepancies still exist between the experimental data and the available theories. These discrepancies are believed to be mainly caused by various flow field assumptions made by different investigators. Even though the problem has been studied both theoretically and experimentally by a number of investigators, it is still unclear at present as to the applicable theory for the different flow regimes. The difficulty of the flow field (3D with strong secondary motion) makes it very difficult to calculate the particle trajectories and deposition in the bend. Unfortunately, detail experiments have not been performed so far for solid-liquid flow excluding experiments for aerosol particles deposition in the bend [8,12], to be validated with this study. This study would be partially validated with the experimental [9] results.

The motivation for this study is to investigate the deposition of solid spherical particles with specific gravity 1.64 as it occurs in water supply network (South East Water Ltd, Melbourne) around bends for a test loop (figure 1). This test loop was investigated by Clive et al [9] in collaboration with South East Water Ltd. The secondary phases of such flows consist of particles with diameters ranging from 2 μm to approximately 20 μm for different velocities. The Eulerian description of turbulence and the role of turbulent structures in the dispersion of particles give us a better understanding in the relationship between temporal and spatial properties of turbulent flows.

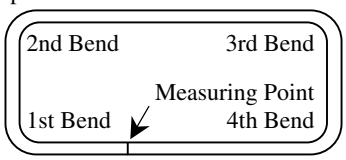

Figure 1: Schematic diagram of the pipe loop with four 90^0 bends.

To study the hydrodynamics of particles behavior in a turbulent flow field numerically: a geometry (figure 1) comprising 41 m long and 100 mm diameter pipe, close-loop with four 90^0 bends has been considered with the boundary conditions shown in table 1 that were used in the experiment [9].

Pipe loop length (m)	41.0
Diameter of the pipe D (m)	0.1
Total volume of water (m^3)	0.322
No. of phases	6
VF of each secondary phases	332×10^{-6} (332 ppm)
Pump	true axial flow
Average water velocities (ms^{-1})	0.05, 0.1, 0.2, 0.3, and 0.4
Particle density (kgm^{-3})	1640
Particles sizes (μm)	2, 5, 10, 15, and 20
No of computational cells	129654

Table 1: Physical and hydraulic characteristics of the system used for CFD simulation.

Governing Equation

The Multiphase Mixture Model of FLUENT 6.1 [6] used in this study solves the continuity and the momentum equation for the mixture. Volume fraction equations are solved for the secondary phases. The model also solves for the well-known algebraic expressions for the relative velocities for secondary phases [7 Chapter 20].

Continuity Equation for the Mixture

The continuity equation for the mixture is

$$\frac{\partial}{\partial t}(\rho_m) + \nabla \cdot (\rho_m \vec{v}_m) = 0 \tag{1}$$

where $\vec{v}_m$ is the mass-averaged velocity:

$$\vec{v}_m = \frac{\sum_{k=1}^{n} \alpha_k \rho_k \vec{v}_k}{\rho_m} \tag{2}$$

and μ_m is the mixture density:

$$\rho_m = \sum_{k=1}^{n} \alpha_k \rho_k \tag{3}$$

α_k is the volume fraction of phase k.

Momentum Equation for the Mixture

The momentum equation for the mixture can be obtained by summing the individual momentum equations for all phases. It can be expressed as:

$$\frac{\partial}{\partial t}(\rho_m \vec{v}_m) + \nabla \cdot (\rho_m \vec{v}_m \vec{v}_m) = -\nabla p + \nabla \cdot \left[\mu_m (\nabla \vec{v}_m + \nabla \vec{v}_m^T)\right] + \rho_m \vec{g} + \vec{F} + \nabla \cdot \left(\sum_{k=1}^{n} \alpha_k \rho_k \vec{v}_{dr,k} \vec{v}_{dr,k}\right) \tag{4}$$

where n is the number of phases, $\vec{F}$ is a body force, and μ_m is the viscosity of the mixture:

$$\mu_m = \sum_{k=1}^{n} \alpha_k \mu_k \tag{5}$$

$\vec{v}_{dr,k}$ is the drift velocity for secondary phase k:

$$\vec{v}_{dr,k} = \vec{v}_k - \vec{v}_m \tag{6}$$

Relative (Slip) Velocity and the Drift Velocity

The relative velocity (also referred to as the slip velocity) is defined as the velocity of a secondary phase (p) relative to the velocity of the primary phase (q):

$$\vec{v}_{qp} = \vec{v}_p - \vec{v}_q \tag{7}$$

The drift velocity and the relative velocity ($\vec{v}_{qp}$) are connected by the following expression:

$$\vec{v}_{dr,p} = \vec{v}_{qp} - \sum_{k=1}^{n} \frac{\alpha_k \rho_k}{\rho_m} \vec{v}_{qk} \tag{8}$$

The basic assumption of the algebraic slip mixture model is that, to prescribe an algebraic relation for the relative velocity, a local equilibrium between the phases should be reached over short spatial length scales. The form of the relative velocity is given by

$$\vec{v}_{qp} = \tau_{qp} \vec{a} \tag{9}$$

where $\vec{a}$ is the secondary-phase particle's acceleration and τ_{qp} is the particulate relaxation time. Following Manninen et al. [16] τ_{qp} is of the form:

$$\tau_{qp} = \frac{(\rho_m - \rho_p) d_p^2}{18 \mu_q f_{drag}} \tag{10}$$

where d_p is the diameter of the particles of secondary phases p, and the drag function f_{drag} is taken from Schiller and Naumann [18]:

$$f_{drag} = \begin{cases} 1 + 0.15 \mathrm{Re}^{0.687} & \mathrm{Re} \le 1000 \\ 0.0183 \mathrm{Re} & \mathrm{Re} > 1000 \end{cases} \tag{11}$$

and the acceleration $\vec{a}$ is of the form

$$\vec{a} = \vec{g} - (\vec{v}_m \cdot \nabla)\vec{v}_m - \frac{\partial \vec{v}_m}{\partial t} \tag{12}$$

The simplest algebraic slip formulation is the so-called drift flux model, in which the acceleration of the particle is given by gravity and/or a centrifugal force and the particulate relaxation time is modified to take into account the presence of other particles.

Volume Fraction Equation for the Secondary Phases

From the continuity equation for secondary phase p, the volume fraction equation for secondary phase p can be obtained:

$$\frac{\partial}{\partial t}(\alpha_p \rho_p) + \nabla \cdot (\alpha_p \rho_p \vec{v}_m) = -\nabla \cdot (\alpha_p \rho_p \vec{v}_{dr,p}) \tag{13}$$

Turbulence Viscosity (The Spalart-Allmaras Model)

Instead of μ_m (equation 5) the turbulent viscosity, μ_t, is computed from

$$\mu_t = \rho_m \tilde{\nu} f_{v1} \tag{14}$$

where the viscous damping function, f_{v1}, is given by

$$f_{v1} = \frac{\chi^3}{\chi^3 + C_{v1}^3} \tag{15}$$

where $C_{v1} = 7.1$ and

$$\chi \equiv \frac{\tilde{\nu}}{\nu} \tag{16}$$

Results and Discussion

Model Validation: In this paper the results have been validated with the experimental result conducted by Clive et al [9]. At CSIRO Clive et al [9] demonstrated an experiment for particle distribution and deposition in a test loop. In order to compare with the experiment results [9] we have used the same geometry and boundary conditions (table 1). Figure 2 represents the cumulative particle volume fraction (summation of all different size particles) as a function of heights across the pipe at a certain location in the loop for both experiment and CFD results. Figure 2 shows the comparison between experimental and CFD results.

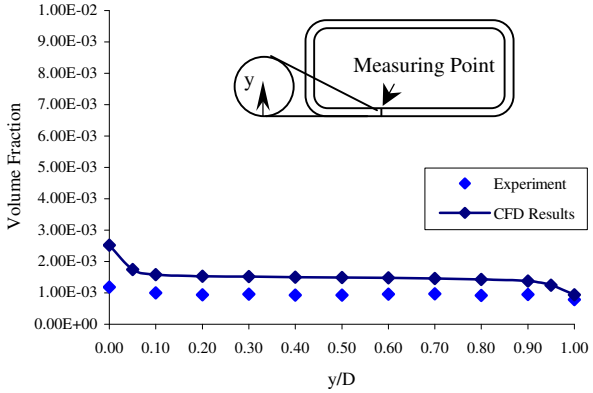

Figure 2: Comparison of CFD results and experimental data [9] for the velocity 0.4 ms^{-1} at center of the pipe.

Nevertheless, the trend is similar, but the experimental results show marginally lower volume fraction. This is because of the shortcomings of the measuring instruments that used in the experiment. Clive et al [9] reported that particle larger than 20 µm could not be detected by the instruments although small amount of particles larger than 20 µm still were introduced into the system. Those larger particles, which tend to settle quickly at the bottom, were also out of count during experiment. This may be the cause of lower volume fraction at the very bottom.

Discussion

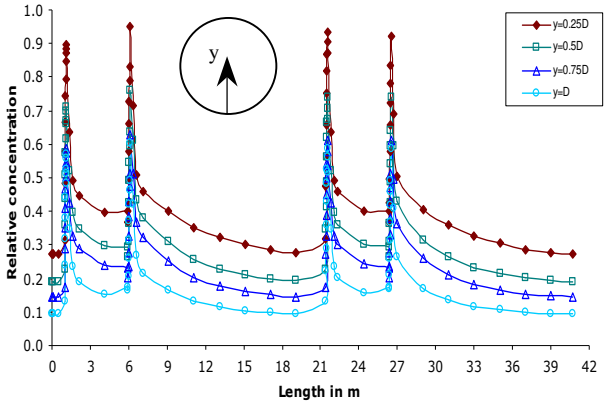

Figure 3a: Relative concentration of particles for different depths along the pipe at 0.05 ms^{-1}.

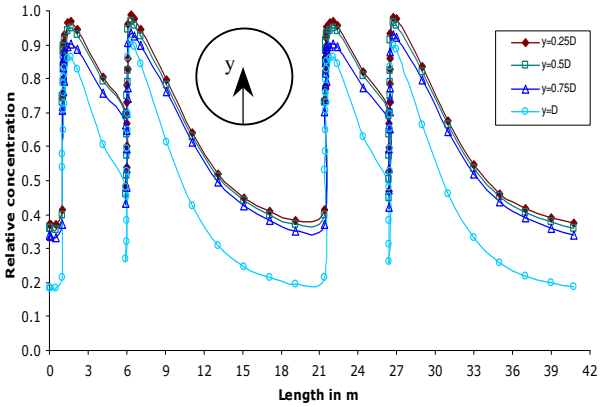

Figure 3b: Relative concentration of particles for different depths along the pipe at 0.4 ms^{-1}.

Figures 3a and 3b show the relative concentration plotted along the pipe for different height of 0.25D, 0.5D, 0.75D, and 1D from the bottom wall of the pipe. Relative concentration is a dimensionless parameter, which represents the ratio of local particle concentration to that of bottom of the pipe wall. Figures 3a and 3b show more homogeneous distribution of particles at different depths in the bend region. Due to high steam line curvature and associated centrifugal force the fluid at different depths gets well mixed resulting in homogeneous distribution of particles near bend. Down stream of the bend, the streamline curvature and associated centrifugal force disappears and particles start to segregate to different concentration at different depths. This segregation or stratification is more pronounced at lower velocity. At higher velocity the particles do not get enough time to segregate before they reach the next bend. Higher turbulence at higher velocity also contributes to homogeneity of the particles around bends.

Figures 4a-4b show typical circumferential distributions of particles volume fraction for the different velocities (0.05 and 0.4 ms^{-1}) for up and downstream location of bends (1st, 3rd and 4th). The angle 0^0 starts at the top wall and angle 180^0 is the bottom wall of the pipe. The upstream profiles exhibit a distinctive variation with the maximum deposition at the bottom of the pipe. Similar trends for entry of the bends were observed from the experimental data of Anderson & Russell [2] and the analytical results of Mols and Oliemans [17] and Laurinat et al [13] and Hossain et al [10]. The peak deposition at the bottom wall is high when the velocity is low. This can be easily explained as particles disperse at higher velocity and can be found higher concentration across the cross-section of the pipe due to high turbulence [13,17]. However, the trends of the particle deposition at upstream of bends (figures 4a-4b) are not symmetrical along vertical plane. This is because of the particles entrainment in between bends is governed by the particle distribution of previous upstream bend, which is different from straight pipe flow [11,13,17].

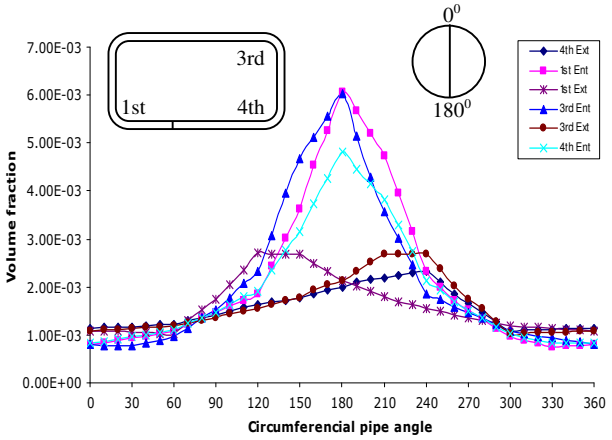

Figure 4a: Cumulative particle deposition (CFD) as a function of circumferential pipe angles at three different up and down stream of bends at 0.05 ms^{-1}.

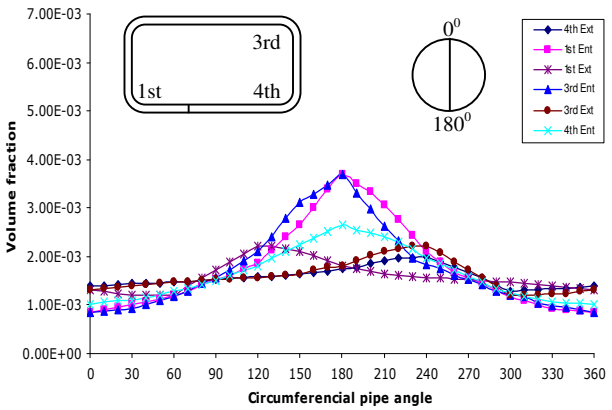

Figure 4b: Cumulative particle deposition (CFD) as a function of circumferential pipe angles at three different up and down stream of bends at 0.4 ms^{-1}.

As shown in figures 4a-4b at downstream of the bend the maximum deposition does not occur at the bottom (180^0) rather it occurs at on the inner wall of the bend. The location of the peak deposition is situated at an angular displacement of 60^0 with respect to the bottom of the wall. The fluid is subjected to centrifugal force as it flows around the bend. Particles having higher specific gravity get segregation and deposit in the bend region. This deposition is pronounced near the outer wall of the bend entry and inner wall of the bend exit. However, due to the influence of high particle distribution at the inner wall upstream bend exit, the inner wall of the downstream bend entry will receive relatively higher load of particles.

In figures (5a-5b) the volume fraction of particles plotted as a function of circumferential angles for different planes (0^0, 22.5^0, 45^0, 67.5^0, and 90^0) of 4th bend (figure 1) for different velocities (0.05 and 0.4 ms^{-1}). 0^0 and 90^0 planes are known also as up and down stream planes respectively. The peak deposition (figures 5a-5b) moves from bottom (180^0) to 240^0 (60^0 inner wall from bottom) as it goes from upstream plane (0^0) to downstream plane (90^0). For a higher velocity (figure 5b), the particle diffusivity increases as a result of fluid diffusivity, which resulted in less particles deposition at the bottom inner wall.

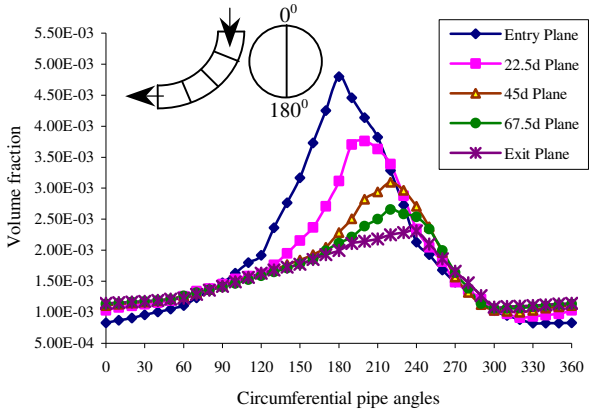

Figure 5a: Particle deposition (CFD) as a function of circumferential pipe angles at different planes of 4th bend at 0.05 ms^{-1}.

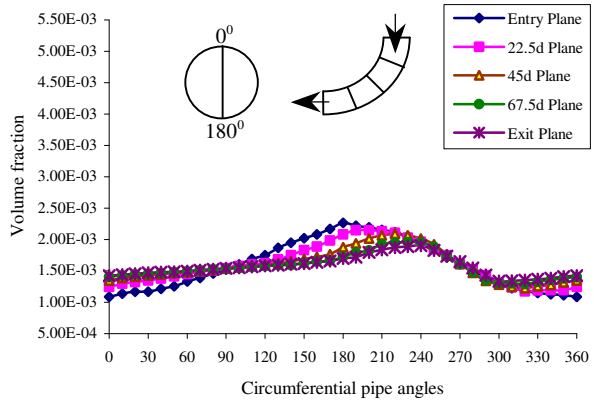

Figure 5b: Particle deposition (CFD) as a function of circumferential pipe angles at different planes of 4th bend at 0.4 ms^{-1}.

Conclusion

The effect of bend and velocities on the deposition of particle in a horizontal test loop (figure 1) has been investigated numerically. This CFD results have also been validated with the experimental results [9] shown in figure 2. A reasonably good agreement between simulation and experiment results has also been established. Relative deposition at various velocities (figures 3a and 3b) indicates that particles are evenly distributed at bends. The circumferential particle deposition for different planes of a bend has also been investigated. Near and around the bends the maximum deposition of particles does not occur at bottom (180^0) rather it occurs at 60^0 skewed to the inner wall. The further study would be needed to conclude more comprehensively the particle deposition around periphery at the downstream of bend.

References

[1] Abuzeid, S., Busniana, A. A., and Ahmadi, G., Wall deposition of aerosol particles in a turbulent channel flow, *Journal of Aerosol Science*, **22**, 1991.

[2] Anderson, R. J. and Russell, T. W. F., Circumferential variation of interchange in horizontal annular two-phase flow, *Ind. Engg. Chem. Fundam.*, **9**, 1970.

[3] Anderson, R. J. and Russell, T. W. F., Film formation in two-phase annular flow, *AIChE Jl*, **14**, 1970, 626-633.

[4] David, Y. H. P., Francisco Romay-Novas, and Benjamin Y. H. Liu, Experimental study of particle deposition in bends of circular cross section, *Aerosol Science and Technology*, **7**, 1987, 301-315..

[5] C.N. Davies. *Aerosol Science*, London, Academic Press, 1966.

[6] FLUENT INC., FLUENT, *ver. 6.1.22, rel*. 2001. USA.

[7] FLUENT INC. FLUENT *Manual. In: Anonymous* USA: 2001.

[8] Friendlander, S. K. and Johnstone, H. F., Deposition of suspended particles from turbulent gas streams, *Industrial and Engineering Chemistry*, **49**, 1957, 1151.

[9] Grainger, C., Wu, J., Nguyen, B. V., Ryan, G., Jayanratne, A., and Mathes, P., Part 1: Settling , Re-Suspension and Transport, CRC, CFC, Melbourne, Australia, Apr 2003.

[10] Hossain, A. , Naser, J., and McManus, A. M. K., Analytical turbulent diffusion model for particle dispersion and deposition in a horizontal pipe flow: comparison with CFD simulation, *Journal of Hydraulic Engineering*, (submitted)

[11] Hossain, A., Naser, J., McManus, A. M. K., and Ryan, G., CFD Investigation of particle deposition and dispersion in a horizontal Pipe, *Third International Conference on CFD in the Minerals and Process Industries*, Dec. 2003.

[12] Landahl, H. D. and Herrmann, R. G., *Journal of Colloid and Interface Science*, **4**, 1949.

[13] Laurinat, J. E., Hanratty, T. J., and Jepson, W. P., Film thickness distribution for gas-liquid annular flow in a horizontal pipe, *Phys. Chem. Hydrodynam.*, **6**, 1985, 179-195.

[14] Li, A. and Ahmadi, G., Deposition of aerosols on surfaces in a turbulent channel flow, *International Journal of Engineering and Science*, **31**, 1993.

[15] Liu, B. Y. H. and Agarwal, J. K., Experimental observation of aerosol deposition in turbulent flows, *Journal of Aerosol Science*, **5**, 1974, 145.

[16] Manninen, M., Taivassalo, V., and Kallio, S., On the mixture model for multiphase flow, *VTT Publications 288*, Technical Research Centre of Finland., 1996.

[17] Mols, B. and Oliemans, R. V. A., A Turbulent diffusion model for particle dispersion and deposition in horizontal tube flow, *International Journal of Multiphase Flow*, **24**, 1998, 55-75.,.

[18] Schiller, L. and Nuamann, Z., *Z.Ver. Deutsch. Ing*., **77**, 1935, 318.

[19] Swailes, D. C. and Reeks, M. W., Particle deposition from a turbulent flow. I. A steady-state model for high inertia particles. *Physics of Fluids*, **6**, 1994, 3392.

[20] Thomson, D. J., Dispersion of particle pairs and decay of scalar fields in isotropic turbulence. *Physics of Fluids*, **15**, 2003, 801-813.

[21] Tsai, C. J. and Pui, D. Y. H., Numerical study of particle deposition in bends of a circular cross section laminar flow regime, *Aerosol Science and Technology*, **12**, 1990.